



TECH BRIEFS

NATIONAL AERONAUTICS AND SPACE ADMINISTRATION

-  **Technology Focus**
-  **Electronics/Computers**
-  **Software**
-  **Materials**
-  **Mechanics**
-  **Machinery/Automation**
-  **Manufacturing & Prototyping**
-  **Bio-Medical**
-  **Physical Sciences**
-  **Information Sciences**
-  **Books and Reports**

INTRODUCTION

Tech Briefs are short announcements of innovations originating from research and development activities of the National Aeronautics and Space Administration. They emphasize information considered likely to be transferable across industrial, regional, or disciplinary lines and are issued to encourage commercial application.

Availability of NASA Tech Briefs and TSPs

Requests for individual Tech Briefs or for Technical Support Packages (TSPs) announced herein should be addressed to

National Technology Transfer Center

Telephone No. (800) 678-6882 or via World Wide Web at www2.nttc.edu/leads/

Please reference the control numbers appearing at the end of each Tech Brief. Information on NASA's Innovative Partnerships Program (IPP), its documents, and services is also available at the same facility or on the World Wide Web at <http://ipp.nasa.gov>.

Innovative Partnerships Offices are located at NASA field centers to provide technology-transfer access to industrial users. Inquiries can be made by contacting NASA field centers listed below.

NASA Field Centers and Program Offices

Ames Research Center

Lisa L. Lockyer
(650) 604-1754
lisa.l.lockyer@nasa.gov

Dryden Flight Research Center

Gregory Poteat
(661) 276-3872
greg.poteat@dfrc.nasa.gov

Goddard Space Flight Center

Nona Cheeks
(301) 286-5810
nona.k.cheeks@nasa.gov

Jet Propulsion Laboratory

Ken Wolfenbarger
(818) 354-3821
james.k.wolfenbarger@jpl.nasa.gov

Johnson Space Center

Michele Brekke
(281) 483-4614
michele.a.brekke@nasa.gov

Kennedy Space Center

David R. Makufka
(321) 867-6227
david.r.makufka@nasa.gov

Langley Research Center

Martin Waszak
(757) 864-4052
martin.r.waszak@nasa.gov

Glenn Research Center

Robert Lawrence
(216) 433-2921
robert.f.lawrence@nasa.gov

Marshall Space Flight Center

Vernotto McMillan
(256) 544-2615
vernotto.mcmillan@msfc.nasa.gov

Stennis Space Center

John Bailey
(228) 688-1660
john.w.bailey@nasa.gov

Carl Ray, Program Executive

Small Business Innovation
Research (SBIR) & Small
Business Technology
Transfer (STTR) Programs
(202) 358-4652
carl.g.ray@nasa.gov

Merle McKenzie

Innovative Partnerships
Program Office
(202) 358-2560
merle.mckenzie-1@nasa.gov



TECH BRIEFS

NATIONAL AERONAUTICS AND SPACE ADMINISTRATION



5 Technology Focus: Data Acquisition

- 5 Inferring Gear Damage From Oil-Debris and Vibration Data
- 6 Forecasting of Storm-Surge Floods Using ADCIRC and Optimized DEMs
- 7 User Interactive Software for Analysis of Human Physiological Data
- 8 Representation of Serendipitous Scientific Data



9 Electronics/Computers

- 9 Automatic Locking of Laser Frequency to an Absorption Peak
- 10 Self-Passivating Lithium/Solid Electrolyte/Iodine Cells
- 11 Four-Quadrant Analog Multipliers Using G⁴-FETs
- 12 Noise Source for Calibrating a Microwave Polarimeter
- 13 Hybrid Deployable Foam Antennas and Reflectors
- 14 Coating MCPs With AlN and GaN
- 15 Domed, 40-cm-Diameter Ion Optics for an Ion Thruster
- 16 Gesture-Controlled Interfaces for Self-Service Machines



17 Software

- 17 Dynamically Alterable Arrays of Polymorphic Data Types

- 17 Identifying Trends in Deep Space Network Monitor Data
- 17 Predicting Lifetime of a Thermomechanically Loaded Component
- 17 Partial Automation of Requirements Tracing
- 18 Automated Synthesis of Architecture of Avionic Systems
- 18 SSRL Emergency Response Shore Tool



19 Materials

- 19 Wholly Aromatic Ether-Imides as n-Type Semiconductors
- 20 Carbon-Nanotube-Carpet Heat-Transfer Pads



23 Manufacturing & Prototyping

- 23 Pulse-Flow Microencapsulation System
- 24 Automated Low-Gravitation Facility Would Make Optical Fibers



25 Physical Sciences

- 25 Alignment Cube With One Diffractive Face



27 Books & Reports

- 27 Graphite Composite Booms With Integral Hinges
- 27 Tool for Sampling Permafrost on a Remote Planet
- 27 Special Semaphore Scheme for UHF Spacecraft Communications

This document was prepared under the sponsorship of the National Aeronautics and Space Administration. Neither the United States Government nor any person acting on behalf of the United States Government assumes any liability resulting from the use of the information contained in this document, or warrants that such use will be free from privately owned rights.



Inferring Gear Damage From Oil-Debris and Vibration Data

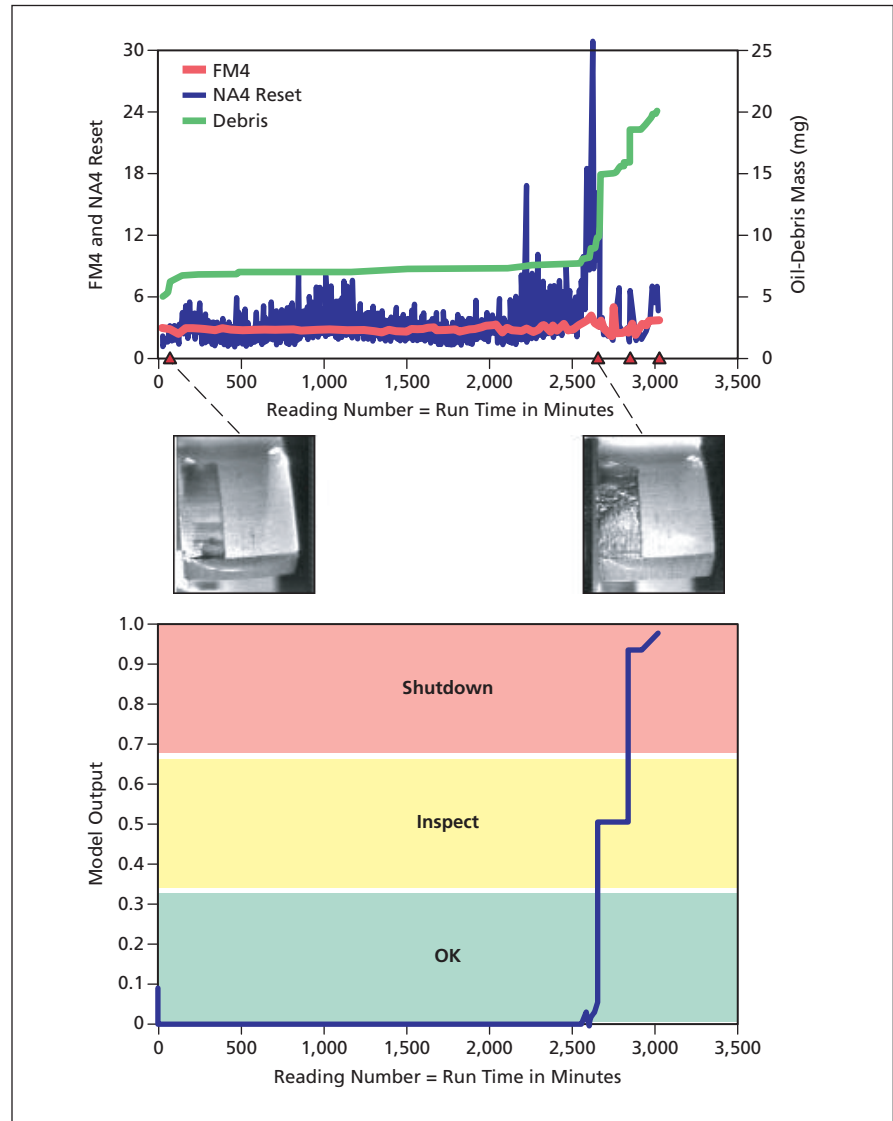
Data fusion increases the reliability and reduces the difficulty of gear-damage diagnosis.

John H. Glenn Research Center, Cleveland, Ohio

A system for real-time detection of surface-fatigue-pitting damage to gears for use in a helicopter transmission is based on fuzzy-logic used to fuse data from sensors that measure oil-borne debris, referred to as “oil debris” in the article, and vibration signatures. A system to detect helicopter-transmission gear damage is beneficial because the power train of a helicopter is essential for propulsion, lift, and maneuvering, hence, the integrity of the transmission is critical to helicopter safety. To enable detection of an impending transmission failure, an ideal diagnostic system should provide real-time monitoring of the “health” of the transmission, be capable of a high level of reliable detection (with minimization of false alarms), and provide human users with clear information on the health of the system without making it necessary for them to interpret large amounts of sensor data.

One of the main ideas underlying the present development is that by integrating oil-debris and vibration sensor subsystems into a single diagnostic system, wherein the data from the two types of sensors are appropriately fused, it is possible to make the damage-detection and decision-making capabilities of the resulting diagnostic system better than those of a diagnostic system that incorporates only one of the sensor subsystems. This idea was tested in 24 experiments in NASA Glenn Research Center’s Spur Gear Fatigue Rig, wherein vibrations were measured by two accelerometers and oil debris were measured by a commercially available inductance-type oil-debris sensor. Speed and load were also measured. The vibration and speed data were processed by two gear diagnostic algorithms that yielded temporally varying statistical parameters known in the art as “FM4” and “NA4 Reset,” respectively.

Multisensor-data-fusion analysis techniques were applied to the FM4, NA4 Reset, and oil-debris data. Data from the different sensors were combined to make inferences that could not be made on the basis of data from a single sensor. Such a process is similar to the process in which



These Vibration (FM4 and NA4 Reset) and Oil-Debris Data and the corresponding output of the data-fusion model are the products of one of the experiments performed to test key parts of the developmental diagnostic system.

a human integrates data from multiple sources and senses to make decisions.

Sensor data can be fused at the raw data level, feature level, or decision level. In this development, the decision level was chosen because it does not limit the fusion process to a specific feature or sensor. The FM4 and NA4 Reset parameters and the accumulated mass

of the debris were the features selected for use as input to the data-fusion part of the system. Fuzzy logic was used to identify the damage level indicated by each feature and to perform decision-level fusion on the features. The resulting data-fusion model was capable of discriminating between the stages of pitting wear. The output of the data-fusion model was

in the form of parameters indicating which of three discrete conditions represents the current state of damage and the corresponding action recommended to end users. The three condition/action combinations were denoted “OK” (no damage and no action necessary), “inspect” (initial pitting), and “shutdown” (severe pitting).

The upper part of the figure depicts the FM4, NA4 Reset, and oil-debris data from one experiment during which pitting damage occurred. The lower part of the figure shows the corresponding out-

put of the data-fusion model. Readings were taken once per minute. The triangles indicate when the gear was inspected for damage. As shown in the photograph connected to the second triangle, damage began to occur at approximately reading 2,669 during this experiment. Analysis of the data collected during this and the other experiments confirmed the expectation that it is advantageous to fuse features of data obtained through different sensors and that, as desired, the output of the data-fusion model amounts to clear, reliable information that can be

used in making decisions about the health of the affected gears.

This work was done by Paula Dempsey of Glenn Research Center. Further information is contained in a TSP (see page 1).

*Inquiries concerning rights for the commercial use of this invention should be addressed to:
NASA Glenn Research Center
Innovative Partnerships Office
Attn: Steve Fedor
Mail Stop 4-8
21000 Brookpark Road
Cleveland, Ohio 44135.
Refer to LEW-17889-1.*

Forecasting of Storm-Surge Floods Using ADCIRC and Optimized DEMs

Maximum water levels are mapped for Hurricanes Camille and Katrina.

Stennis Space Center, Mississippi

Increasing the accuracy of storm-surge flood forecasts is essential for improving preparedness for hurricanes and other severe storms and, in particular, for optimizing evacuation scenarios. An interactive database, developed by WorldWinds, Inc., contains atlases of storm-surge flood levels for the Louisiana/Mississippi gulf coast region. These atlases were developed to improve forecasting of flooding along the coastline and estuaries and in adjacent inland areas. Storm-surge heights depend on a complex interaction of several factors, including: storm size, central minimum pressure, forward speed of motion, bottom topography near the point of landfall, astronomical tides, and, most importantly, maximum wind speed.

The information in the atlases was generated in over 100 computational simulations, partly by use of a parallel-processing version of the ADvanced CIRCulation (ADCIRC) model. ADCIRC is a nonlinear computational model of hydrodynamics, developed by the U.S. Army Corps of Engineers and the US Navy, as a family of two- and three-dimensional finite-element-based codes. It affords a capability for simulating tidal circulation and storm-surge propagation over very large computational domains, while simultaneously providing high-resolution output in areas of complex shoreline and bathymetry. The ADCIRC finite-element grid for this project covered the Gulf of Mexico and contiguous basins, extending into the deep Atlantic Ocean with progressively higher resolution approaching the study area. The advantage of using ADCIRC over other

storm-surge models, such as SLOSH, is that input conditions can include all or part of wind stress, tides, wave stress, and river discharge, which serve to make the model output more accurate.

To keep the computational load manageable, this work was conducted using only the wind stress, calculated by using historical data from Hurricane Camille, as the input condition for the model. Hurricane storm-surge simulations were performed on an eight-node Linux computer cluster. Each node contained dual 2-GHz processors, 2GB of memory, and a 40GB hard drive. The digital elevation

model (DEM) for this region was specified using a combination of Navy data (over water), NOAA data (for the coastline), and optimized Interferometric Synthetic Aperture Radar data (over land). This high-resolution topographical data of the Mississippi coastal region provided the ADCIRC model with improved input with which to calculate improved storm-surge forecasts.

Also used in the simulations was a commercially developed rainfall inundation model that originated in research performed for a NASA dual-use project. The rainfall model accepts as input an eleva-

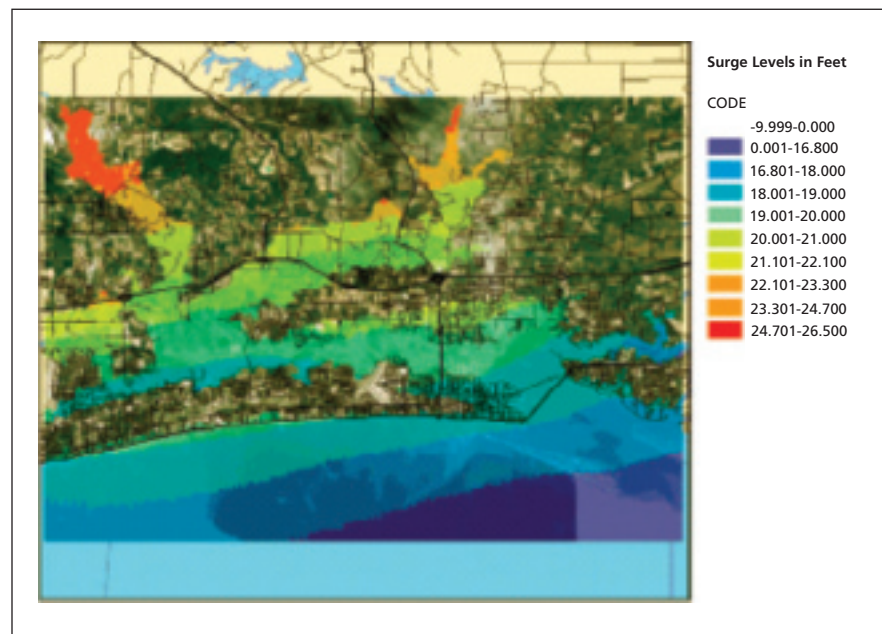


Figure 1. This MEOW Map shows the maximum storm surge at each finite-element node based on all simulations of category-3 hurricanes in the affected area.

tion grid, coordinates to a source cell, and the desired inundation level. Software utilities that accompany the model translate United States Geological Survey digital elevation maps, as well as ASCII grids, into the correct format. The source cell is specified in the coordinates of the elevation grid, and the inundation level (a floating-point number) is specified in a unit of measurement compatible with that used for the input elevation. The rainfall simulations were performed for various hurricane landfall scenarios that included different intensities, storm sizes, forward speeds, and landfall locations.

Typically, each hurricane simulation, started 3 days of simulated time before Camille's landfall, took about 5 hours of computing time in parallel processing on all sixteen processors. The results of the ADCIRC and rainfall simulations were composited to determine the highest storm-surge value possible for each grid node; the resulting maps are known as maximum envelope of water (MEOW) maps.

Figure 1 shows the maximum storm surge for a Category 3 storm in the vicinity of the back bay of Biloxi, MS. The maximum storm surge is approximately 20 ft (≈ 6 m) inside the bay. Over most of the bay area, the storm surge varies between 15 and 25 ft (≈ 4.5 and 7.6 m). Published ground measurements at various discrete locations during Hurricane Camille show that a maximum storm surge of over 22 ft (≈ 6.7 m) occurred at Pass Christian, MS, west of Biloxi. Emergency planners and local government officials make public evacuation plans based on MEOW maps.

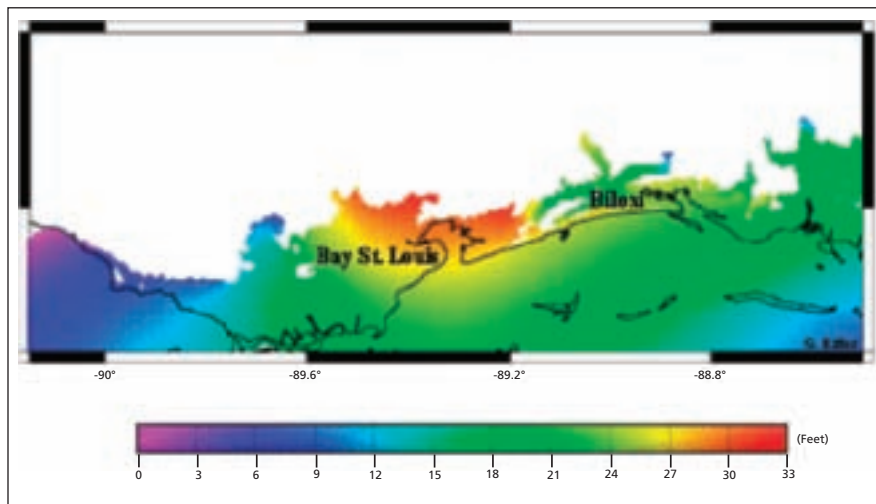


Figure 2. ADCIRC Calculated Storm-Surge Heights for Hurricane Katrina on August 29, 2005, at 11 a.m. local time. This image shows a 25- to 30-ft (≈ 4.5 - to 9.1-m) storm surge in the Bay St. Louis and Pass Christian communities.

Figure 2 depicts ADCIRC computer model simulation of Hurricane Katrina's storm surge, showing a 25- to 30-ft (≈ 4.5 - to 9.1-m) wall of water, pushed by 140-mph (≈ 225 -km/h) winds, slamming into the Louisiana/Mississippi Gulf Coast. The maximum surge from Katrina was higher than Camille and covered a wider region, even though the intensity of the wind was slightly less. This happened because Katrina's strong winds covered a larger area and Katrina moved more slowly than Camille, allowing more time for the water to accumulate.

At the time of this reporting, technical support and parallel-computing resources have been provided to the Louisiana Department of Natural Resources, one private

firm, and NASA, to model hurricane storm-surge flooding in southeastern Louisiana and along the Mississippi Gulf Coast.

This work was done by Elizabeth Valenti and Patrick Fitzpatrick of WorldWinds, Inc. for Stennis Space Center.

In accordance with Public Law 96-517, the contractor has elected to retain title to this invention. Inquiries concerning rights for the commercial use should be addressed to:

*WorldWinds, Inc.
Stennis Space Center
Building 1103, Suite 213C
Stennis Space Center, MS 39529
Phone No.: (228) 688-1468*

Refer to SSC-00229, volume and number of this NASA Tech Briefs issue, and the page number.

User Interactive Software for Analysis of Human Physiological Data

Ames Research Center, Moffett Field, California

Ambulatory physiological monitoring has been used to study human health and performance in space and in a variety of Earth-based environments (e.g., military aircraft, armored vehicles, small groups in isolation, and patients). Large, multi-channel data files are typically recorded in these environments, and these files often require the removal of contaminated data prior to processing and analyses.

Physiological data processing can now be performed with user-friendly, interactive software developed by the Ames Psychophysiology Research Laboratory. This software, which runs on a Windows

platform, contains various signal-processing routines for both time- and frequency-domain data analyses (e.g., peak detection, differentiation and integration, digital filtering, adaptive thresholds, Fast Fourier Transform power spectrum, auto-correlation, etc.). Data acquired with any ambulatory monitoring system that provides text or binary file format are easily imported to the processing software.

The application provides a graphical user interface where one can manually select and correct data artifacts utilizing linear and zero interpolation and adding

trigger points for missed peaks. Block and moving average routines are also provided for data reduction. Processed data in numeric and graphic format can be exported to Excel. This software, PostProc (for post-processing) requires the Dadisp engineering spreadsheet (DSP Development Corp), or equivalent, for implementation. Specific processing routines were written for electrocardiography, electroencephalography, electromyography, blood pressure, skin conductance level, impedance cardiography (cardiac output, stroke volume, thoracic fluid volume), temperature, and respiration.

PostProc users do not need programming experience or extensive knowledge of human electrophysiological signal processing. Routines written in Series Processing Language (SPL) can be modified to accommodate different

biomedical instruments, calibration levels, or sampling rates.

This program was written by Patricia S. Cowings and William Toscano of Ames Research Center and Bruce C. Taylor and Soumydipta Acharya of the University of

Akron. Further information is contained in a TSP (see page 1).

Inquiries concerning rights for the commercial use of this invention should be addressed to the Ames Technology Partnerships Division at (650) 604-2954. Refer to ARC-15287-1.

Representation of Serendipitous Scientific Data

NASA's Jet Propulsion Laboratory, Pasadena, California

A computer program defines and implements an innovative kind of data structure than can be used for representing information derived from serendipitous discoveries made via collection of scientific data on long exploratory spacecraft missions. Data structures capable of collecting any kind of data can easily be implemented in advance, but the task of designing a fixed and efficient data structure suitable for processing raw data into useful information and taking advantage of serendipitous scientific discovery is be-

coming increasingly difficult as missions go deeper into space. The present software eases the task by enabling definition of arbitrarily complex data structures that can adapt at run time as raw data are transformed into other types of information. This software runs on a variety of computers, and can be distributed in either source code or binary code form. It must be run in conjunction with any one of a number of Lisp compilers that are available commercially or as shareware. It has no specific memory requirements

and depends upon the other software with which it is used. This program is implemented as a library that is called by, and becomes folded into, the other software with which it is used.

This program was written by Mark James of Caltech for NASA's Jet Propulsion Laboratory. Further information is contained in a TSP (see page 1).

This software is available for commercial licensing. Please contact Karina Edmonds of the California Institute of Technology at (626) 395-2322. Refer to NPO-42086.



Automatic Locking of Laser Frequency to an Absorption Peak

Initial manual tuning is ordinarily not necessary.

Langley Research Center, Hampton, Virginia

An electronic system adjusts the frequency of a tunable laser, eventually locking the frequency to a peak in the optical absorption spectrum of a gas (or of a Fabry-Perot cavity that has an absorption peak like that of a gas). This system was developed to enable precise locking of the frequency of a laser used in differential absorption LIDAR measurements of trace atmospheric gases. This system also has great commercial potential as a prototype of means for precise control of frequencies of lasers in future dense wavelength-division-multiplexing optical communications systems.

The operation of this system is completely automatic: Unlike in the operation of some prior laser-frequency-locking systems, there is ordinarily no need for a human operator to adjust the frequency manually to an initial value close enough to the peak to enable au-

tomatic locking to take over. Instead, this system also automatically performs the initial adjustment.

The system (see Figure 1) is based on a concept of (1) initially modulating the laser frequency to sweep it through a spectral range that includes the desired absorption peak, (2) determining the derivative of the absorption peak with respect to the laser frequency for use as an error signal, (3) identifying the desired frequency [at the very top (which is also the middle) of the peak] as the frequency where the derivative goes to zero, and (4) thereafter keeping the frequency within a locking range and adjusting the frequency as needed to keep the derivative (the error signal) as close as possible to zero.

More specifically, the system utilizes the fact that in addition to a zero crossing at the top of the absorption peak, the error

signal also closely approximates a straight line in the vicinity of the zero crossing (see Figure 2). This vicinity is the locking range because the linearity of the error signal in this range makes it useful as a source of feedback for a proportional + integral + derivative control scheme that constantly adjusts the frequency in an effort to drive the error to zero. When the laser frequency deviates from the mid-peak value but remains within the locking range, the magnitude and sign of the error signal indicate the amount of detuning and the control circuitry adjusts the frequency by what it estimates to be the negative of this amount in an effort to bring the error to zero.

Before the laser frequency can be locked as described above, it is necessary to find the locking range. For this purpose, the frequency is swept through a broad range that includes the locking range and, in ad-

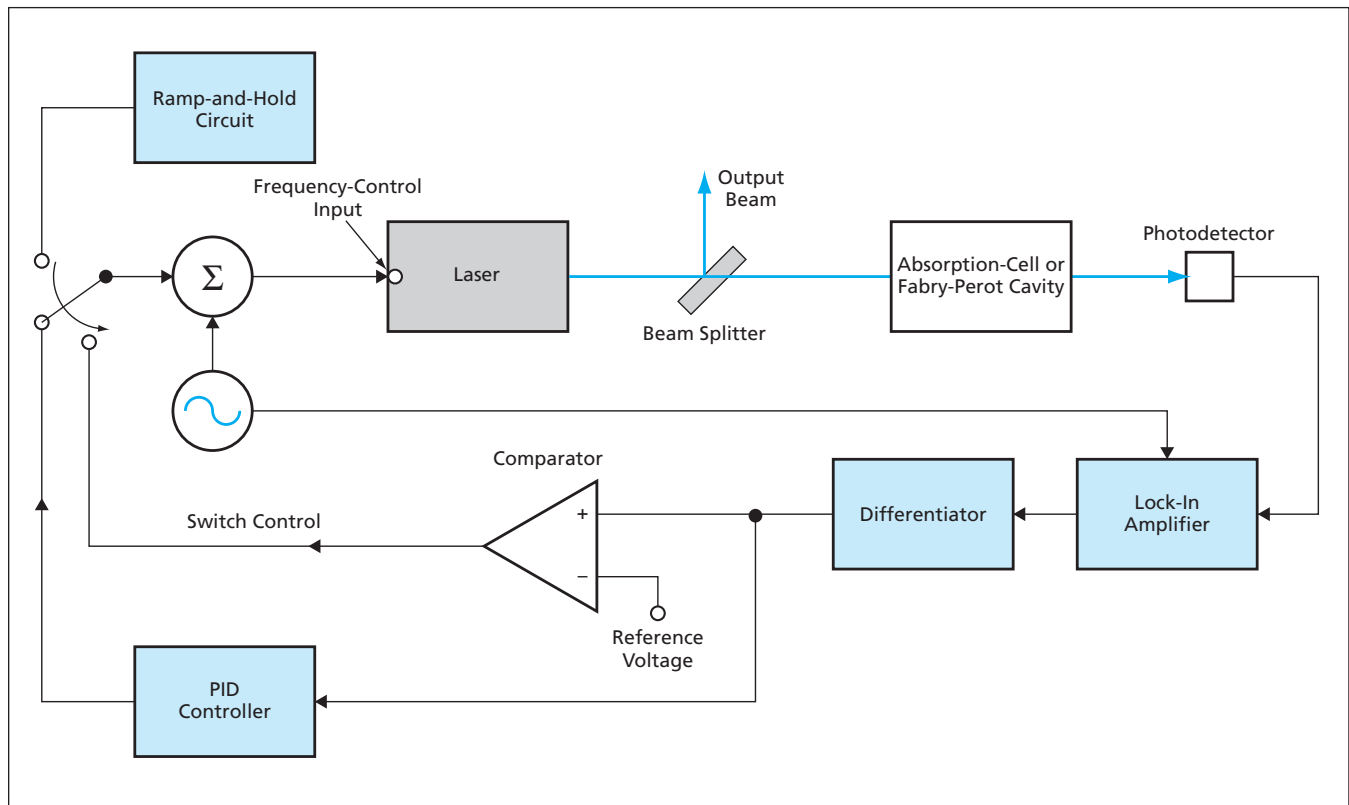


Figure 1. The **Automatic Frequency-Locking System** first sweeps the laser frequency through a wide range to find the locking range, then switches to a locking mode, in which it constantly adjusts the frequency to keep it at the middle of the locking range. (Note: PID is Proportional-Integral-Differential.)

dition to determining the error signal (the first derivative of absorption with respect to frequency), the system also determines the derivative of the error signal with respect to time. The system can readily identify the locking zone because the derivative of the error signal is positive and reaches its highest value in the locking zone and is negative just outside the locking zone. Once the laser frequency is inside the locking zone, the frequency sweep is halted and the frequency-stabilization circuitry that implements the locking scheme described above is activated. In a test, the system was demonstrated to be capable of maintaining the frequency of a diode laser at the middle of a 944-nm-wavelength water-vapor absorption peak, with an error of no more than 3 percent of the full width at half maximum of the peak.

This work was done by Grady J. Koch of Langley Research Center. Further information is contained in a TSP (see page 1). LAR-16394-1

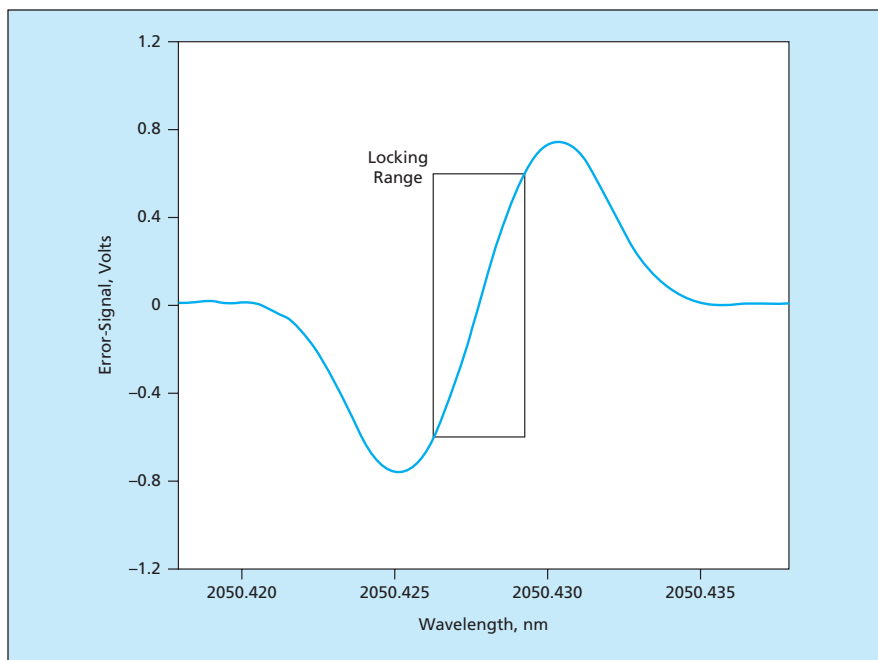


Figure 2. The Error Signal and its derivative are used in finding the locking range and then maintaining lock. This error signal was obtained in operation using a CO₂ absorption peak centered at a wavelength of 2,050.428 nm.

Self-Passivating Lithium/Solid Electrolyte/Iodine Cells

Passivating lithium iodide films of optimum or nearly optimum thickness form spontaneously.

NASA's Jet Propulsion Laboratory, Pasadena, California

Robust lithium/solid electrolyte/iodine electrochemical cells that offer significant advantages over commercial lithium/iodine cells have been developed. At room temperature, these cells can be discharged at current densities 10 to 30 times those of commercial lithium/iodine cells. Moreover, from room temperature up to 80 °C, the maximum discharge-current densities of these cells exceed those of all other solid-electrolyte-based cells.

A cell of this type includes a metallic lithium anode in contact with a commercial flexible solid electrolyte film that, in turn, is in contact with an iodine/graphite cathode. The solid electrolyte (the chemical composition of which has not been reported) offers the high ionic conductivity needed for high cell performance. However, the solid electrolyte exhibits an undesirable chemical reactivity to lithium that, if not mitigated, would render the solid electrolyte unsuitable for use in a lithium cell. In this cell, such mitigation is affected by the formation of a thin passivating layer of lithium iodide at the anode/electrolyte interface.

Test cells of this type were fabricated from iodine/graphite cathode pellets, free-standing solid-electrolyte films, and

lithium-foil anodes. The cathode mixtures were made by grinding together blends of nominally 10 weight percent graphite and 90 weight percent iodine. The cathode mixtures were then pressed into pellets at 36 kpsi (248 MPa) and inserted into coin-shaped stainless-steel cell cases that were coated with graphite paste to minimize corrosion. The solid-electrolyte film material was stamped to form circular pieces to fit in the coin cell cases, inserted in the cases, and pressed against the cathode pellets with polyethylene gaskets. Lithium-foil anodes were placed directly onto the electrolyte films. The layers described thus far were pressed and held together by stainless-steel shims, wave springs, and coin cell caps. The assembled cells were then crimped to form hermetic seals.

It was found that the solid electrolyte films became discolored within seconds after they were placed in contact with the cathodes — a result of facile diffusion of iodine through the solid electrolyte material (see figure). This is fortuitous for the following reasons:

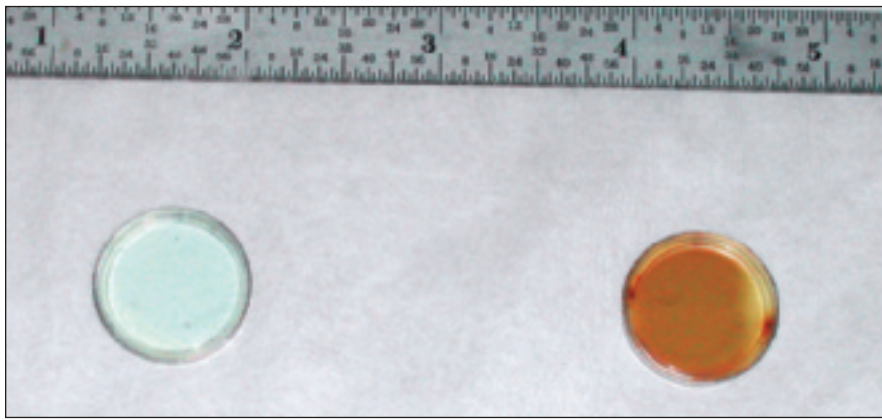
- Upon reaching the anode side, the iodine reacts with lithium from the anode to form lithium iodide, which is known as both a solid electrolyte and an effec-

tive passivating-film material for solid electrolytes in contact with lithium.

- Heretofore, it has been necessary to vacuum-deposit LiI onto a solid electrolyte to form a passivating film. The vacuum-deposition process is expensive, time-consuming, and difficult. If the thickness of the deposited LiI film is ≈ 1 mm or more, the high electrical resistivity of LiI limits the cell discharge rates. If the film is too thin, it likely contains pinholes, which act as corrosion sites and thereby degrade cell performance.
- In the present case, the LiI is neither thick enough to introduce excessive electrical resistance nor too thin to prevent formation of pinholes: The formation of LiI film is self-limiting because iodine diffuses very slowly through LiI.

Commercial lithium/iodine cells are primary cells (that is, they are not rechargeable, as opposed to secondary cells, which are rechargeable). Thus far, lithium/solid-electrolyte/iodine cells have been demonstrated in primary form only. However, in principle, the present approach to passivation should be applicable to secondary cells also.

This work was done by Ratnakumar Bugga, Jay Whitacre, Sekharipuram Narayanan, and



The **Half Cell** on the left contains a graphite cathode pellet behind a solid-electrolyte film. The half cell on the right contains a graphite/iodine pellet behind a solid-electrolyte film; the darkening of this cell was caused by diffusion of iodine through the solid electrolyte.

William West of Caltech for NASA's Jet Propulsion Laboratory. Further information is contained in a TSP (see page 1).

In accordance with Public Law 96-517, the contractor has elected to retain title to this invention. Inquiries concerning rights for its commercial use should be addressed to:

Innovative Technology Assets Management
JPL

Mail Stop 202-233
4800 Oak Grove Drive
Pasadena, CA 91109-8099
(818) 354-2240

E-mail: iaoffice@jpl.nasa.gov

Refer to NPO-40789, volume and number of this NASA Tech Briefs issue, and the page number.

Four-Quadrant Analog Multipliers Using G^4 -FETs

Devices with independently biased multiple inputs are exploited to simplify multiplier circuits.

NASA's Jet Propulsion Laboratory, Pasadena, California

Theoretical analysis and some experiments have shown that the silicon-on-insulator (SOI) 4-gate transistors known as G^4 -FETs can be used as building blocks of four-quadrant analog voltage multiplier circuits. Whereas a typical prior analog voltage multiplier contains between six and 10 transistors, it is possible to construct a superior voltage multiplier using only four G^4 -FETs.

A G^4 -FET is a combination of a junction field-effect transistor (JFET) and a metal oxide/semiconductor field-effect transistor (MOSFET). It can be regarded as a single transistor having four gates, which are parts of a structure that affords high functionality by enabling the utilization of independently biased multiple inputs. The structure of a G^4 -FET of the type of interest here (see Figure 1) is that of a

partially-depleted SOI MOSFET with two independent body contacts, one on each side of the channel. The drain current comprises of majority charge carriers flowing from one body contact to the other — that is, what would otherwise be the side body contacts of the SOI MOSFET are used here as the end contacts [the drain (D) and the source (S)] of the G^4 -FET. What would otherwise be the

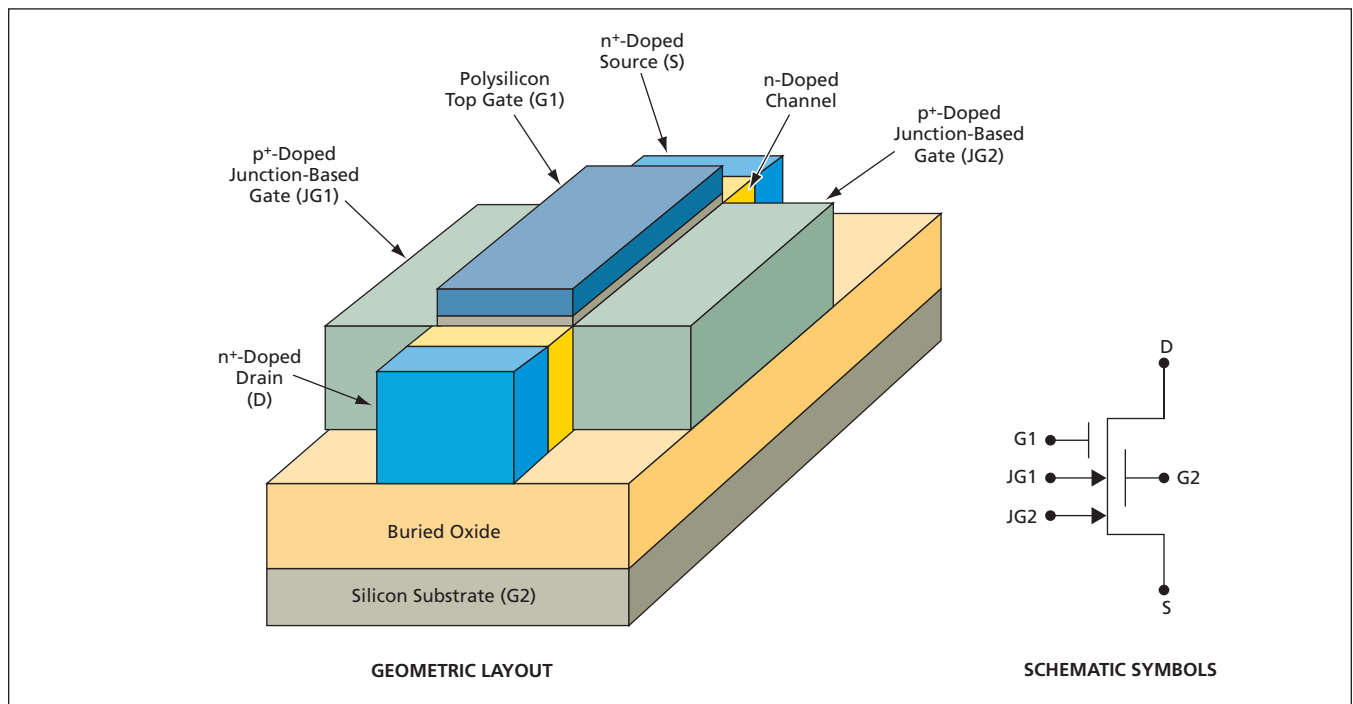


Figure 1. In this G^4 -FET, the top gate plays the same role as does the sole gate in a conventional accumulation-mode MOSFET. The side gates (JG1 and JG2) provide additional degrees of freedom for design and operation, beyond those of a conventional MOSFET.

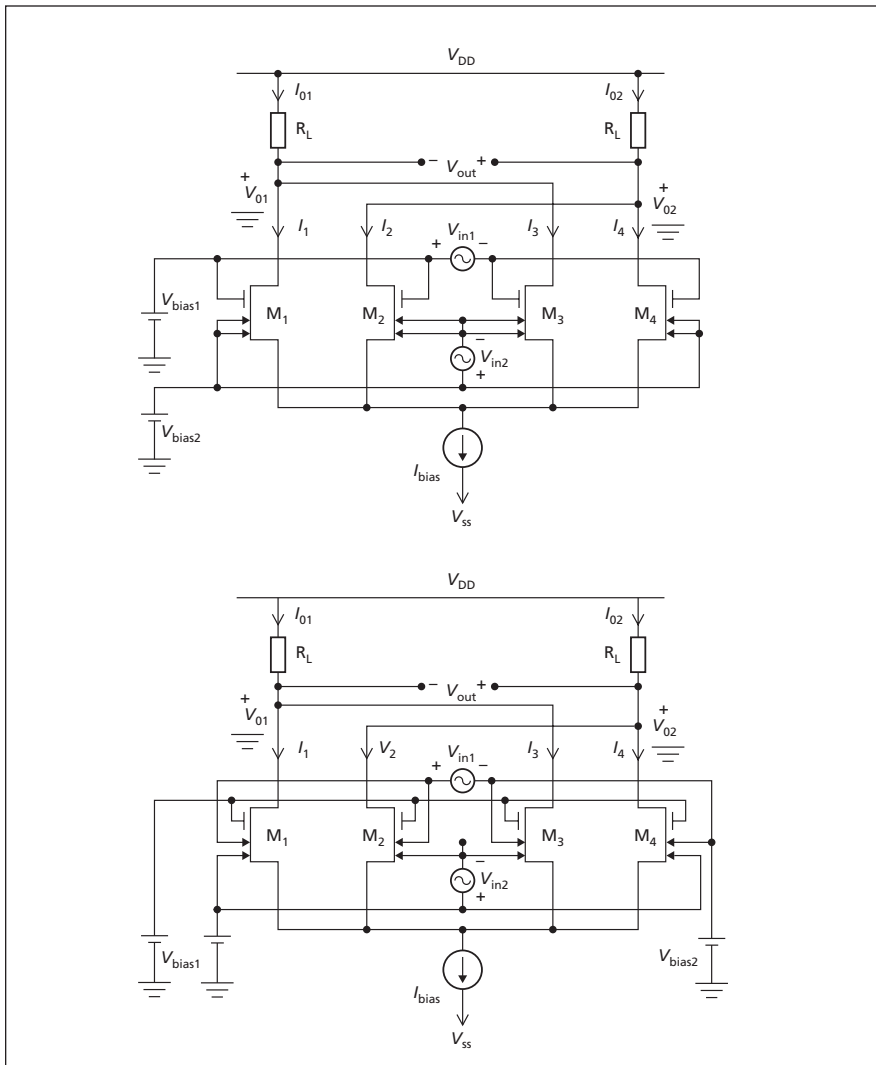


Figure 2. These **Two G⁴-FET Analog Multiplier Circuits** are examples of implementation of four-quadrant multipliers using fewer transistors than were previously required for such multipliers.

source and drain of the SOI MOSFET serve, in the G⁴-FET, as two junction-based extra gates (JG1 and JG2), which are used to squeeze the channel via reverse-biased junctions as in a JFET. The G⁴-FET also includes a polysilicon top gate (G1), which plays the same role as does the gate in an accumulation-mode MOSFET. The substrate emulates a fourth MOS gate (G2).

By making proper choices of G⁴-FET device parameters in conjunction with

bias voltages and currents, one can design a circuit in which two input gate voltages (V_{in1}, V_{in2}) control the conduction characteristics of G⁴-FETs such that the output voltage (V_{out}) closely approximates a value proportional to the product of the input voltages. Figure 2 depicts two such analog multiplier circuits. In each circuit, there is the following:

- The input and output voltages are differential,

- The multiplier core consists of four G⁴-FETs (M1 through M4) biased by a constant current sink (I_{bias}), and
- The G⁴-FETs in two pairs are loaded by two identical resistors (R_L), which convert a differential output current to a differential output voltage.

The difference between the two circuits stems from their input and bias configurations. In each case, provided that the input voltages remain within their design ranges as determined by considerations of bias, saturation, and cutoff, then the output voltage is nominally given by $V_{out} = k V_{in1} V_{in2}$, where k is a constant gain factor that depends on the design parameters and is different for the two circuits.

In experimental versions of these circuits constructed using discrete G⁴-FETs and resistors, multiplication of voltages in all four quadrants (that is, in all four combinations of input polarities) was demonstrated, and deviations of the output voltages from linear dependence on the input voltages were found to amount to no more than a few percent. It is anticipated that in fully integrated versions of these circuits, the deviations from linearity will be made considerably smaller through better matching of devices.

This work was done by Mohammad Mojaradi, Benjamin Blalock, Sorin Christoloveanu, Suheng Chen, and Kerem Akarvardar of Caltech for NASA's Jet Propulsion Laboratory. Further information is contained in a TSP (see page 1).

In accordance with Public Law 96-517, the contractor has elected to retain title to this invention. Inquiries concerning rights for its commercial use should be addressed to:

*Innovative Technology Assets Management
JPL*

*Mail Stop 202-233
4800 Oak Grove Drive
Pasadena, CA 91109-8099
(818) 354-2240*

E-mail: iaoffice@jpl.nasa.gov

Refer to NPO-41586, volume and number of this NASA Tech Briefs issue, and the page number.

🌊 Noise Source for Calibrating a Microwave Polarimeter

This compact unit can readily be integrated into an airborne microwave instrumentation.

Goddard Space Flight Center, Greenbelt, Maryland

A correlated-noise source has been developed for use in calibrating an airborne or spaceborne Earth-observing correlation microwave polarimeter that

operates in a pass band that includes a nominal frequency of 10.7 GHz. Deviations from ideal behavior of the hardware of correlation polarimeters are

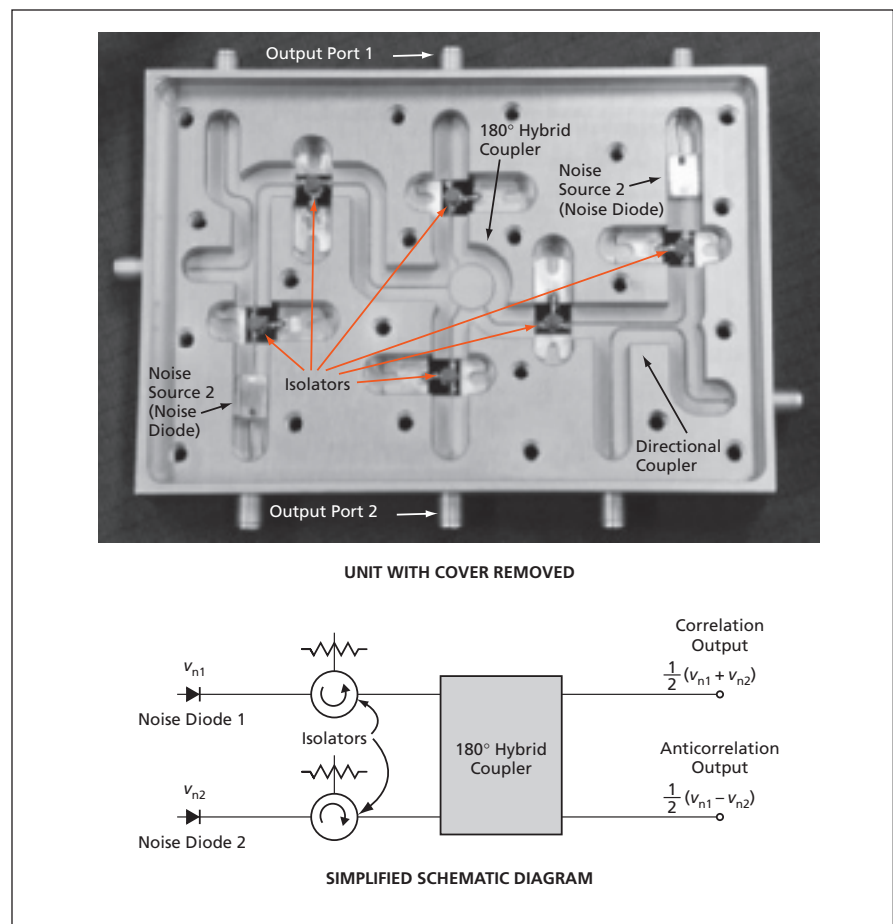
such as to decorrelate the signals measured by such an instrument. A correlated-noise source provides known input signals, measurements of which can be

processed to estimate and correct for the decorrelation effect.

Typical prior correlated-noise sources suitable for this purpose consist of multiple units connected by coaxial cables; as such, they tend to be too bulky and heavy to be incorporated into flight instrumentation assemblies. In contrast, the present correlated-noise source is a single unit (see figure) that is relatively compact and can easily be integrated into a flight instrumentation assembly. The unit includes directional couplers for sampling noise-diode outputs and injection of test signals. This source provides both correlated (sum) and anticorrelated (difference) signal components at the output ports. The source can be operated in four modes: (1) both noise diodes on, (2) both noise diodes off, (3) noise diode 1 on with noise diode 2 off, and (4) noise diode 2 on with noise diode 1 off. Measurements of the resulting combinations of correlated and anticorrelated signal components provide the data needed for calibration.

This work was done by Jeffrey R. Piepmeier and Edward J. Kim of Goddard Space Flight Center. Further information is contained in a TSP (see page 1).

This invention is owned by NASA, and a patent application has been filed. Inquiries concerning nonexclusive or exclusive license for its commercial development should be addressed to the Patent Counsel, Goddard Space Flight Center, (301) 286-7351. Refer to GSC-14745-1.



This **Correlated-Noise Source** includes noise diodes and microstrip components in a single, integral housing. Adherence to geometric tolerances of circuit layout, with special attention to considerations of symmetry, is essential for proper operation.

Hybrid Deployable Foam Antennas and Reflectors

Compressed foam structures would be expanded to full size and shape.

NASA's Jet Propulsion Laboratory, Pasadena, California

Hybrid deployable radio antennas and reflectors of a proposed type would feature rigid narrower apertures plus wider adjoining apertures comprising reflective surfaces supported by open-cell polymeric foam structures (see figure). The open-cell foam structure of such an antenna would be compressed for compact stowage during transport. To initiate deployment of the antenna, the foam structure would simply be released from its stowage mechanical restraint. The elasticity of the foam would drive the expansion of the foam structure to its full size and shape.

There are several alternatives for fabricating a reflective surface supported by a polymeric foam structure. One approach would be to coat the foam with a metal. Another approach would be to attach a metal film or a metal-coated polymeric

membrane to the foam. Yet another approach would be to attach a metal mesh to the foam.

The hybrid antenna design and deployment concept as proposed offers significant advantages over other concepts for deployable antennas:

- In the unlikely event of failure to deploy, the rigid narrow portion of the antenna would still function, providing a minimum level of assured performance. In contrast, most other concepts for deploying a large antenna from compact stowage are of an "all or nothing" nature: the antenna is not useful at all until and unless it is fully deployed.
- Stowage and deployment would not depend on complex mechanisms or actuators, nor would it involve the use of in-

flatable structures. Therefore, relative to antennas deployed by use of mechanisms, actuators, or inflation systems, this antenna could be lighter, cheaper, amenable to stowage in a smaller volume, and more reliable.

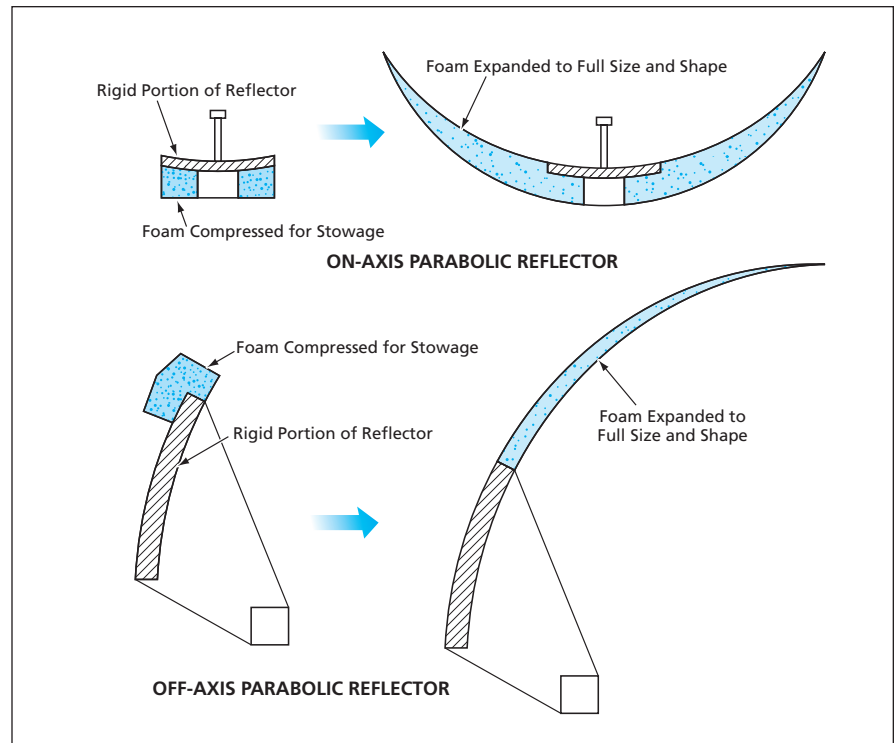
An open-cell polymeric (e.g., polyurethane) foam offers several advantages for use as a compressible/expandable structural material to support a large antenna or reflector aperture. A few of these advantages are the following:

- The open cellular structure is amenable to compression to a very small volume — typically to 1/20 of its full size in one dimension.
- At a temperature above its glass-transition temperature (T_g), the foam strongly damps vibrations. Even at a temperature below T_g , the damping

should exceed that of other materials.

- In its macroscopic mechanical properties, an open-cell foam is isotropic. This isotropy facilitates computational modeling of antenna structures.
- Through chemical formulation, the T_g of an open-cell polyurethane foam can be set at a desired value between about -100 and about 0 °C. Depending on the application, it may or may not be necessary to rigidify a foam structure after deployment. If rigidification is necessary, then the T_g of the foam can be tailored to exceed the temperature of the deployment environment, in conjunction with providing a heater to elasticize the foam for deployment. Once deployed, the foam would become rigidified by cooling to below T_g .
- Techniques for molding or machining polymeric foams (especially including open-cell polyurethane foams) to desired sizes and shapes are well developed.

This work was done by Tommaso Rivellini, Paul Willis, Richard Hodges, and Suzanne Spitz of Caltech for NASA's Jet Propulsion Laboratory. Further information is contained in a TSP (see page 1). NPO-30819



These On- and Off-Axis Parabolic Reflectors are two examples of antenna reflectors that would include rigid narrow apertures and adjoining deployable foam-supported wider apertures.

Coating MCPs With AlN and GaN

Emission of electrons is increased.

Goddard Space Flight Center, Greenbelt, Maryland

A development effort underway at the time of reporting the information for this article is devoted to increasing the sensitivity of microchannel plates (MCPs) as detectors of photons and ions by coating the MCPs with nitrides of elements in period III of the periodic table. Conventional MCPs are relatively insensitive to slowly moving, large-mass ions — for example, ions of biomolecules under analysis in mass spectrometers. The idea underlying this development is to coat an MCP to reduce its work function (decrease its electron affinity) in order to increase both (1) the emission of electrons in response to impingement of low-energy, large-mass ions and (2) the multiplying effect of secondary electron emission.

Of particular interest as coating materials having appropriately low or even negative electron affinities are gallium nitride, aluminum nitride, and ternary alloys of general composition $Al_xGa_{1-x}N$ (where $0 < x < 1$). These materials exhibit attractively high degrees of chemical, mechanical, and thermal stability plus

acceptably high resistance to sputtering. The electron-excitation cross sections of these materials are expected to exceed those of several other materials (including diamond) that are, variously, in use or under development for the same purpose. Moreover, by doping these materials with silicon, one can render them partly electrically conductive, thereby suppressing the undesired accumulation of electric charge that could otherwise occur during bombardment by ions.

For experiments, thin films of AlN and GaN — both undoped and doped with Si — were deposited on commercial MCPs by radio-frequency molecular-beam epitaxy (also known as plasma-assisted molecular-beam epitaxy) at temperatures < 200 °C. This deposition technique is particularly suitable because (1) MCPs cannot withstand the higher deposition-substrate temperatures used to decompose constituent compounds in some other deposition techniques and (2) in this technique, the constituent Al, Ga, and N are sup-

plied in elemental form, so that there is no need for thermal decomposition at the substrate surface. The nitride films thus formed were, variously, amorphous or polycrystalline. The nitride films were coated with surface layers of gold < 100 Å thick.

The MCPs were tested in a standard configuration in which the output stage of a first MCP was coupled to the input stage of a second MCP. Each pair of MCPs was mounted in a standard holder that included front and back contact rings and an anode for collecting the output electrons of the second MCP. The MCP pairs were biased at potentials between 1.7 and 1.9 kV, and count rates measured after preamplification and discrimination. To enable a direct comparison, in one pair, the second MCP was uncoated while the first MCP was coated over half its surface. The coated and uncoated sides of the half-coated MCP were exposed to fluxes of argon ions at kinetic energies of 1.0 and 0.5 keV. At 1.0 keV, the count rate for the coated side was about 2.3 times greater than

that for the uncoated side; at 0.5 keV, the count rate for the coated side was about 1.8 times greater than that for the uncoated side.

This work was done by Abdelhakim Bensaoula, David Starikov, and Chris Boney of Integrated Micro Sensors, Inc. and Abdelhak Bensaoula of the University of Houston

*for Goddard Space Flight Center. Further information is contained in a TSP (see page 1).
GSC-14936-1*

Domed, 40-cm-Diameter Ion Optics for an Ion Thruster

A modified design affords better performance without loss of service life.

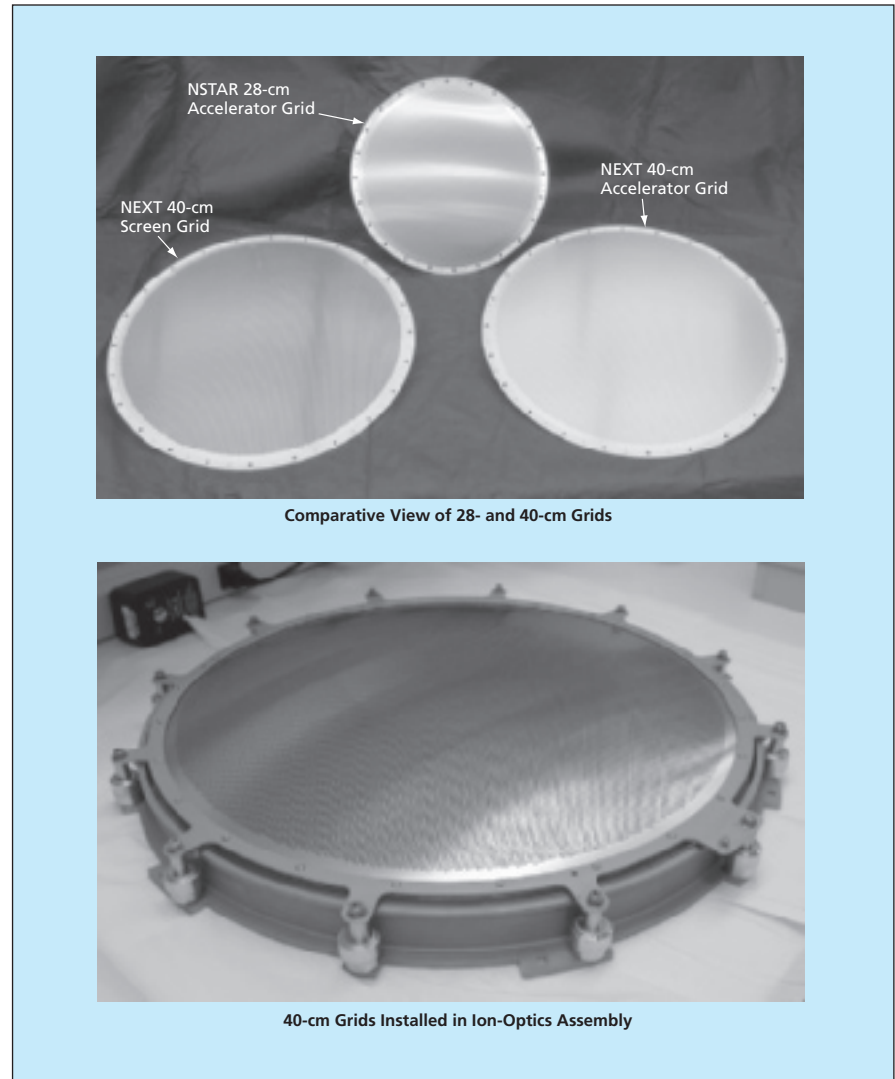
John H. Glenn Research Center, Cleveland, Ohio

Improved accelerator and screen grids for an ion accelerator have been designed and tested in a continuing effort to increase the sustainable power and thrust at the high end of the accelerator throttling range. The accelerator and screen grids are undergoing development for intended use as NASA's Evolutionary Xenon Thruster (NEXT) — a spacecraft thruster that would have an input-power throttling range of 1.2 to 6.9 kW. The improved accelerator and screen grids could also be incorporated into ion accelerators used in such industrial processes as ion implantation and ion milling.

NEXT is a successor to the NASA Solar Electric Propulsion Technology Application Readiness (NSTAR) thruster — a state-of-the-art ion thruster characterized by, among other things, a beam-extraction diameter of 28 cm, a span-to-gap ratio (defined as this diameter divided by the distance between the grids) of about 430, and a rated peak input power of 2.3 kW. To enable the NEXT thruster to operate at the required higher peak power, the beam-extraction diameter was increased to 40 cm — almost doubling the beam-extraction area over that of NSTAR (see figure). The span-to-gap ratio was increased to 600 to enable throttling to the low end of the required input-power range.

The geometry of the apertures in the grids was selected on the basis of experience in the use of grids of similar geometry in the NSTAR thruster. Characteristics of the aperture geometry include a high open-area fraction in the screen grid to reduce discharge losses and a low open-area fraction in the accelerator grid to reduce losses of electrically neutral gas atoms or molecules. The NEXT accelerator grid was made thicker than that of the NSTAR to make more material available for erosion, thereby increasing the service life and, hence, the total impulse.

The NEXT grids are made of molybdenum, which was chosen because its combination of high strength and low



The NEXT 40-cm Grids are dome-shaped as are the 28-cm NSTAR grids.

thermal expansion helps to minimize thermally and inertially induced deflections of the grids. A secondary reason for choosing molybdenum is the availability of a large database for this material. To keep development costs low, the NEXT grids have been fabricated by the same techniques used to fabricate the NSTAR grids. In tests, the NEXT ion optics have been found to outperform the NSTAR ion optics, as expected.

This work was done by George C. Soulas, Thomas W. Haag, and Michael J. Patterson of Glenn Research Center. Further information is contained in a TSP (see page 1).

Inquiries concerning rights for the commercial use of this invention should be addressed to NASA Glenn Research Center, Commercial Technology Office, Attn: Steve Fedor, Mail Stop 4-8, 21000 Brookpark Road, Cleveland, Ohio 44135. Refer to LEW-17598-1.

Gesture-Controlled Interfaces for Self-Service Machines

Potential advantages include immunity to wear and increased safety.

Lyndon B. Johnson Space Center, Houston, Texas

Gesture-controlled interfaces are software-driven systems that facilitate device control by translating visual hand and body signals into commands. Such interfaces could be especially attractive for controlling self-service machines (SSMs) — for example, public information kiosks, ticket dispensers, gasoline pumps, and automated teller machines (see figure).

A gesture-controlled interface would include a vision subsystem comprising one or more charge-coupled-device video cameras (at least two would be needed to acquire three-dimensional images of gestures). The output of the vision system would be processed by a pure software gesture-recognition subsystem. Then a translator subsystem would convert a sequence of recognized gestures into commands for the SSM to be controlled; these could include, for example, a command to display requested information, change control settings, or actuate a ticket- or cash-dispensing mechanism.

Depending on the design and operational requirements of the SSM to be controlled, the gesture-controlled interface could be designed to respond to specific static gestures, dynamic gestures, or both. Static and dynamic gestures can include stationary or moving hand signals, arm poses or motions, and/or whole-body postures or motions. Static gestures would be recognized on the basis of their shapes; dynamic gestures would be recognized on the basis of both their shapes and their motions. Because dynamic gestures include temporal as well as spatial content, this gesture-controlled interface can extract more information from dynamic than it can from static gestures.

Gesture-controlled interfaces offer several advantages over other input devices commonly used in SSMs:

- There would be no mechanical wear because unlike a keyboard, push-button switch, and/or computer mouse, a gesture-controlled interface contains no moving parts.
- Inasmuch as there would be no direct contact with users, there would be no



A User Would Control an Automated Teller Machine through gestures. Panels on the sides of the machine would depict static and dynamic hand and arm signals recognized by the system.

problem of hygiene as there is with a touch screen.

- Unlike a speech-recognition system, a gesture-controlled interface could operate in a noisy location because it does not respond to sound.
- The safety of users of automated teller machines could be increased because the translator subsystems of gesture-controlled interfaces could be made to recognize poses and motions associated with the crimes committed at such machines.
- Systems will be designed to recognize gestures that are natural to users, thereby decreasing the time required to learn how to operate SSMs. The area of an SSM surrounding a display screen could contain pictures of hand signals or other gestures recognized by the system.

- The use of gestures as a communication medium may help to overcome language barriers to the use of SSMs in communities with diverse populations.

This work was done by Charles J. Cohen and Glenn Beach of Cybernet Systems Corp. for Johnson Space Center.

In accordance with Public Law 96-517, the contractor has elected to retain title to this invention. Inquiries concerning rights for its commercial use should be addressed to:

*Cybernet Systems Corporation
727 Airport Boulevard
Ann Arbor, MI 48108
Phone: (734) 668-2567
Fax: (734) 668-8780
Web: www.cybernet.com*

Refer to MSC-23002, volume and number of this NASA Tech Briefs issue, and the page number.



Dynamically Alterable Arrays of Polymorphic Data Types

An application library package was developed that represents data packets for Deep Space Network (DSN) message packets as dynamically alterable arrays composed of arbitrary polymorphic data types. The software was to address a limitation of the present state of the practice for having an array directly composed of a single monomorphic data type. This is a severe limitation when one is dealing with science data in that the types of objects one is dealing with are typically not known in advance and, therefore, are dynamic in nature. The unique feature of this approach is that it enables one to define at run-time the dynamic shape of the matrix with the ability to store polymorphic data types in each of its indices. Existing languages such as C and C++ have the restriction that the shape of the array must be known in advance and each of its elements be a monomorphic data type that is strictly defined at compile-time. This program can be executed on a variety of platforms. It can be distributed in either source code or binary code form. It must be run in conjunction with any one of a number of Lisp compilers that are available commercially or as shareware.

This program was written by Mark James of Caltech for NASA's Jet Propulsion Laboratory. Further information is contained in a TSP (see page 1).

This software is available for commercial licensing. Please contact Karina Edmonds of the California Institute of Technology at (626) 395-2322. Refer to NPO-42071.

Identifying Trends in Deep Space Network Monitor Data

A computer program has been developed that analyzes Deep Space Network monitor data, looking for changes of trends in critical parameters. This program represents a significant improvement over the previous practice of manually plotting data and visually inspecting the resulting graphs to identify trends. This program uses proven numerical techniques to identify trends. When a statistically significant trend is detected, then it is characterized by means of a symbol that can be used by pre-existing

model-based reasoning software. The program can perform any of the following functions:

- Given an expectation that data in a given list should exhibit an upward, downward, constant, or unknown trend, it can determine whether the data do or do not follow such a trend.
- Given a list of data, it can identify which of the aforementioned trends the data follow.
- Given two lists of data, it can determine whether or not both follow the same trend.

This program can be executed on a variety of computers. It can be distributed in either source code or binary code form. It must be run in conjunction with any one of a number of Lisp compilers that are available commercially or as shareware.

This program was written by Mark James of Caltech for NASA's Jet Propulsion Laboratory. Further information is contained in a TSP (see page 1).

This software is available for commercial licensing. Please contact Karina Edmonds of the California Institute of Technology at (626) 395-2322. Refer to NPO-42107.

Predicting Lifetime of a Thermomechanically Loaded Component

NASALIFE is a computer program for predicting the lifetime, as affected by low cycle fatigue (LCF) and creep rupture, of a structural component subject to temporally varying, multiaxial thermomechanical loads. The component could be, for example, part of an aircraft turbine engine. Empirical data from LCF tests, creep rupture tests, and static tensile tests are used as references for predicting the number of missions the component can withstand under a given thermomechanical loading condition.

The user prepares an input file containing the creep-rupture and cyclic-fatigue information, temperature-dependent material properties, and mission loading and control flags. The creep rupture information can be entered in tabular form as stress versus life or by means of parameters of the Larson-Miller equation. The program uses the Walker mean-stress model to adjust predicted life for ranges of the ratio between the

maximum and minimum stresses. Data representing complex load cycles are reduced by the rainflow counting method. Miner's rule is utilized to combine the damage at different load levels. Finally, the program determines the total damage due to creep and combines it with the fatigue damage due to the cyclic loading and predicts the approximate number of missions a component can endure before failing.

This work was done by Pappu L. N. Murthy of Glenn Research Center, John Z. Gyekenyesi of N&R Engineering and Management Services Corp., Subodh Mital of the University of Toledo, and David N. Brewer of the U. S. Army Aviation Systems Command. Further information is contained in a TSP (see page 1).

Inquiries concerning rights for the commercial use of this invention should be addressed to NASA Glenn Research Center, Innovative Partnerships Office, Attn: Steve Fedor, Mail Stop 4-8, 21000 Brookpark Road, Cleveland, Ohio 44135. Refer to LEW-18081.

Partial Automation of Requirements Tracing

Requirements Tracing on Target (RETRO) is software for after-the-fact tracing of textual requirements to support independent verification and validation of software. RETRO applies one of three user-selectable information-retrieval techniques: (1) term frequency/inverse document frequency (TF/IDF) vector retrieval, (2) TF/IDF vector retrieval with simple thesaurus, or (3) keyword extraction. One component of RETRO is the graphical user interface (GUI) for use in initiating a requirements-tracing project (a pair of artifacts to be traced to each other, such as a requirements spec and a design spec). Once the artifacts have been specified and the IR technique chosen, another component constructs a representation of the artifact elements and stores it on disk.

Next, the IR technique is used to produce a first list of candidate links (potential matches between the two artifact levels). This list, encoded in Extensible Markup Language (XML), is optionally processed by a "filtering" component designed to make the list somewhat smaller without sacrificing accuracy. Through the

GUI, the user examines a number of links and returns decisions (yes, these are links; no, these are not links). Coded in XML, these decisions are provided to a “feedback processor” component that prepares the data for the next application of the IR technique. The feedback reduces the incidence of erroneous candidate links. Unlike related prior software, RETRO does not require the user to assign keywords, and automatically builds a document index.

This program was developed by Jane Hayes, Alex Dekhtyar, Senthil Sundaram, and Sravanthi Vadlamudi of the University of Kentucky for Goddard Space Flight Center. Further information is contained in a TSP (see page 1). GSC-14976-1.

Automated Synthesis of Architectures of Avionic Systems

The Architecture Synthesis Tool (AST) is software that automatically synthesizes software and hardware architectures of avionic systems. The AST is expected to be most helpful during initial formulation of an avionic-system design, when system requirements change frequently and manual modification of architecture is time-consuming and susceptible to error. The AST comprises two parts: (1) an architecture generator, which utilizes a genetic algorithm to create a multitude of architectures; and (2) a functionality evaluator, which analyzes the architectures for viability, rejecting most of the non-viable ones. The functionality evaluator gener-

ates and uses a viability tree — a hierarchy representing functions and components that perform the functions such that the system as a whole performs system-level functions representing the requirements for the system as specified by a user. Architectures that survive the functionality evaluator are further evaluated by the selection process of the genetic algorithm. Architectures found to be most promising to satisfy the user’s requirements and to perform optimally are selected as parents to the next generation of architectures. The foregoing process is iterated as many times as the user desires. The final output is one or a few viable architectures that satisfy the user’s requirements.

This program was written by Savio Chau, Joseph Xu, Van Dang, and James F. Lu of Caltech for NASA’s Jet Propulsion Laboratory. Further information is contained in a TSP (see page 1).

This software is available for commercial licensing. Please contact Karina Edmonds of the California Institute of Technology at (626) 395-2322. Refer to NPO-42607.

SSRL Emergency Response Shore Tool

The SSRL Emergency Response Shore Tool (wherein “SSRL” signifies “Smart Systems Research Laboratory”) is a computer program within a system of communication and mobile-computing software and hardware being developed to increase the situational awareness of first responders at building collapses. This program is intended for use mainly

in planning and constructing shores to stabilize partially collapsed structures. The program consists of client and server components, runs in the Windows operating system on commercial off-the-shelf portable computers, and can utilize such additional hardware as digital cameras and Global Positioning System devices.

A first responder can enter directly, into a portable computer running this program, the dimensions of a required shore. The shore dimensions, plus an optional digital photograph of the shore site, can then be uploaded via a wireless network to a server. Once on the server, the shore report is time-stamped and made available on similarly equipped portable computers carried by other first responders, including shore wood cutters and an incident commander. The staff in a command center can use the shore reports and photographs to monitor progress and to consult with structural engineers to assess whether a building is in imminent danger of further collapse.

This program was written by Robert W. Mah, Richard Papsin, Dawn M. McIntosh, Douglas Denham, and Charles Jorgensen of Ames Research Center; Bradley J. Betts of Computer Sciences Corporation; and Rommel Del Mundo of QSS Group, Inc. Further information is contained in a TSP (see page 1).

This invention is owned by NASA and a patent application has been filed. Inquiries concerning rights for the commercial use of this invention should be addressed to the Ames Technology Partnerships Division at (650) 604-2954. Refer to ARC-15461-1.



Wholly Aromatic Ether-Imides as n-Type Semiconductors

Some of the compounds exhibit promising electron-transport properties.

Langley Research Center, Hampton, Virginia

Some wholly aromatic ether-imides consisting of rod-shaped, relatively-low-mass molecules that can form liquid crystals have been investigated for potential utility as electron-donor-type (n-type) organic semiconductors. It is envisioned that after further research to improve understanding of their physical and chemical properties, compounds of this type would be used to make thin-film semiconductor devices (e.g., photovoltaic cells and field-effect transistors) on flexible electronic-circuit substrates.

This investigation was inspired by several prior developments:

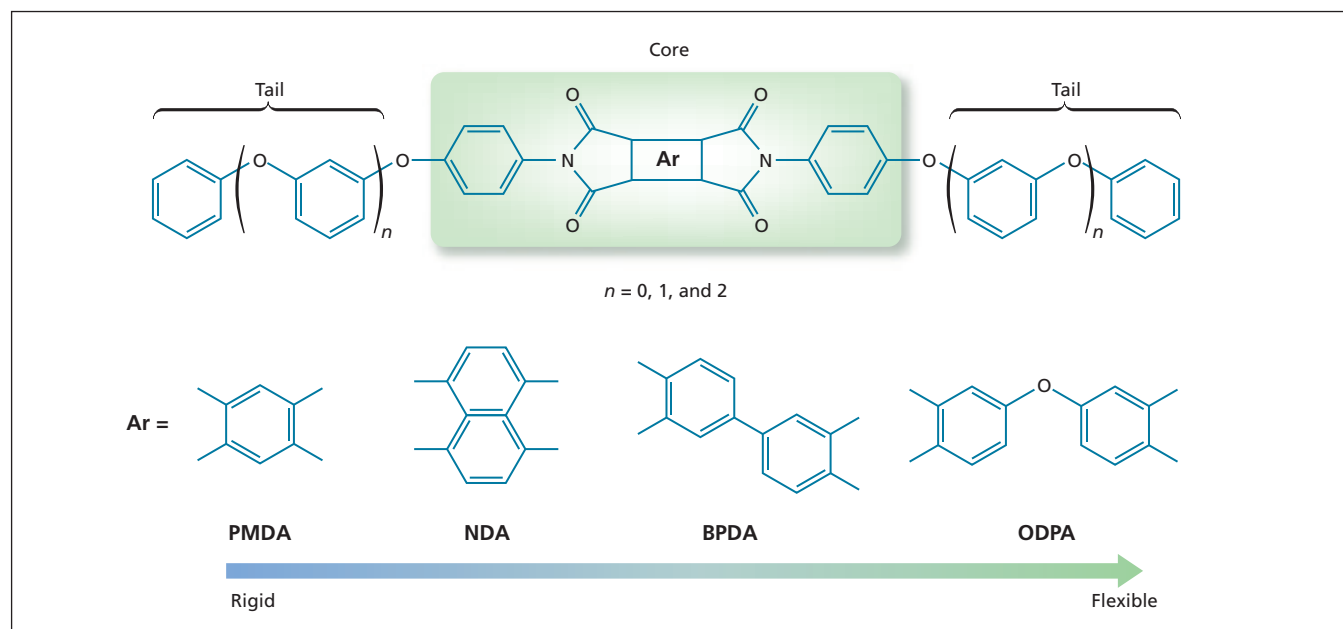
- Poly(ether-imides) [PEIs] are a class of engineering plastics that have been used extensively in the form of films in a variety of electronic applications, including insulating layers, circuit boards, and low-permittivity coatings.
- Wholly aromatic PEIs containing naphthalene and perylene moieties have been shown to be useful as electrochromic polymers.
- More recently, low-molecular-weight imides comprising naphthalene-based molecules with terminal fluorinated tails were shown to be useful as n-type

organic semiconductors in such devices as field-effect transistors and Schottky diodes.

Poly(etherimide)s as structural resins have been extensively investigated at NASA Langley Research Center for over 30 years. More recently, the need for multi-functional materials has become increasingly important. This n-type semiconductor illustrates the scope of current work towards new families of PEIs that not only can be used as structural resins for carbon-fiber reinforced composites, but also can function as sensors. Such a multi-functional material would permit so-called *in-situ* health monitoring of composite structures during service. The work presented here demonstrates that parts of the PEI backbone can be used as an n-type semiconductor with such materials being sensitive to damage, temperature, stress, and pressure. In the near future, multi-functional or "smart" composite structures are envisioned to be able to communicate such important parameters to the flight crew and provide vital information with respect to the operational status of their aircraft.

Prior attempts to make electronic devices based on n-type organic semiconductors had failed because permeation by oxygen from air limited the lifetimes of the devices. In this development, the close molecular packing in the fluorinated imides is believed to have extended the lifetimes and improved the performances of the devices by preventing permeation by oxygen and moisture.

On the basis of promising results in the aforementioned prior developments and of other considerations, it was conjectured that for the purpose of developing n-type organic semiconductors, wholly aromatic imide-based mesogenic (liquid-crystal-forming) compounds would offer several advantages over non-mesogenic compounds. Liquid crystals are well known for their outstanding barrier properties, and when designed properly, their unique packing motifs could result in increased charge-carrier mobilities. Conceivably, rigid aromatic dianhydrides terminated with appropriate aryl-ether amines could have the requisite liquid crystalline properties. Prior to this investigation, some research groups had reported on



Ether-Imide Compounds investigated for utility as n-type semiconductors have this generic molecular structure.

low-molecular-weight imide-based liquid crystals, but these compounds contain aliphatic units, which lack the oxidative stability necessary for semiconductor applications.

The generic molecular structure of the wholly aromatic ether-imide compounds of this investigation is a classic “tail-core-tail” structure, which is denoted by the term “calamitic” in the liquid-crystal art. In the generic molecule, the core contains one of four dianhydrides with a *p*-phenylamine at each end. The dianhydrides are pyromellitic dianhydride (PMDA); 1,4,5,8-naphthalenetetracarboxylic dianhydride (NDA); 3,3',4,4'-biphenyltetracarboxylic dianhydride (BPDA), and 3,3',4,4'-oxydiphthalic dianhydride (ODPA). The tails are members of a homologous series of meta-substituted aryl-ethers. Each tail is the para substituent on the *p*-phenylamine (see figure).

This generic molecular structure was chosen for the following reasons: The *p*-

phenylamine functionality increases the length of the core beyond that of the rigid di-imide portion, while the bulky meta-substituted aryl-ether tails have some flexibility. Increasing the numbers of meta-substituted aryl units in the tails reduces melt transition temperatures and increases solubilities. Also, the tails stabilize the molecular orientations necessary for mesophase formation. Aryl-ether flexible tails had not been used previously as flexible tail segments in liquid crystals, and in comparison with alkyl or alkyloxy flexible tails, aryl-ether tails have more breath, which keeps the overall diameters of mesogens more nearly uniform.

In the investigation, monofunctional amines (destined to become tails) were synthesized by various techniques, then combined with the dianhydrides (destined to become the cores) in one-step solution imidization procedures to obtain the desired ether imides. These compounds were examined for tempera-

ture-dependent phase behavior by means of optical microscopy and x-ray diffraction, and cyclic voltammetry was used to characterize redox behavior. Absorption spectroscopic measurements were also performed on dilute solutions of the compounds. Of these compounds, those containing NDA and BPDA in the cores were found to have electron-transport properties suitable for n-type semiconductors. Of all the compounds tested, only one containing NDA in the core clearly exhibited a tendency toward formation of liquid crystals. This is the first example, known at the time of the tests, in which a mesophase was detected in a wholly aromatic ether-imide compound.

This work was done by Erik Weiser and Terry L. St. Clair of Langley Research Center; Theo J. Dingemans (ICASE); Edward T. Samulski and Gene Irene of the University of North Carolina at Chapel Hill. Further information is contained in a TSP (see page 1). LAR-17041-1

Carbon-Nanotube-Carpet Heat-Transfer Pads

The compliance and high longitudinal thermal conductivity of carbon nanotubes are exploited.

Ames Research Center, Moffett Field, California

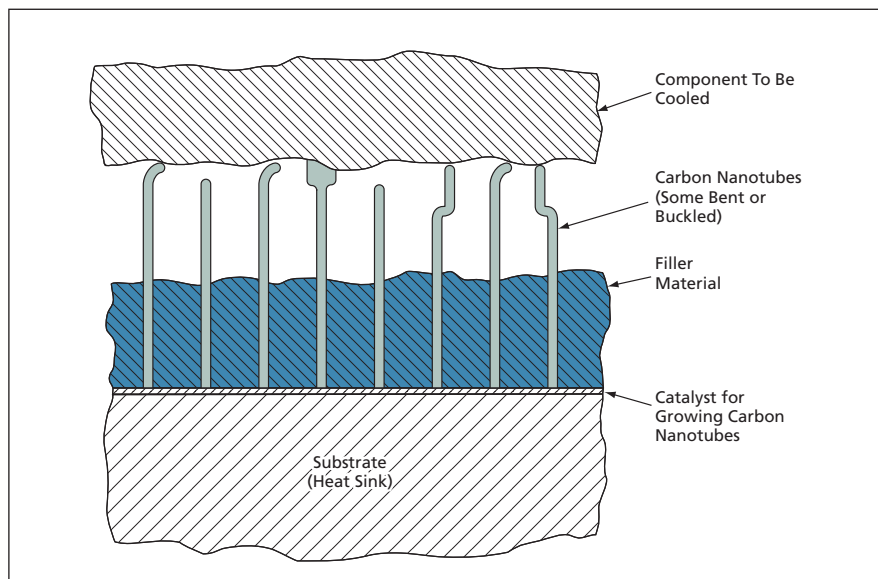
Microscopic thermal-contact pads that include carpetlike arrays of carbon nanotubes have been invented for dissipating heat generated in integrated circuits and similarly sized single electronic components. The need for these or other innovative thermal-contact pads arises because the requisite high thermal conductances cannot be realized by scaling conventional macroscopic thermal-contact pads down to microscopic sizes. Overcoming limitations of conventional thermal-contact materials and components, the carbon-nanotube thermal-contact pads offer the high thermal conductivities needed to accommodate the high local thermal power densities of modern electronic circuits, without need for large clamping pressures, extreme smoothness of surfaces in contact, or gap-filling materials (e.g., thermally conductive greases) to ensure adequate thermal contact. Moreover, unlike some conventional thermal-contact components, these pads are reusable.

The figure depicts a typical pad according to the invention, in contact with a rough surface on an electronic component that is to be cooled. Through reversible bending and buckling of carbon nanotubes at asperities on the rough sur-

face, the pad yields sufficiently, under relatively low contact pressure, that thermal contact is distributed to many locations on the surface to be cooled, including valleys where contact would not ordinarily occur in conventional clamping of rigid surfaces. Hence, the effective thermal-contact

area is greater than that achievable through scaling down of a macroscopic thermal-contact pad.

The extremely high longitudinal thermal conductivities of the carbon nanotubes are utilized to conduct heat away from potential hot spots on the surface to be



Carbon Nanotubes Bend and Buckle to accommodate roughness of the surface of the component to be cooled. The high longitudinal thermal conductivity of carbon nanotubes is exploited to conduct heat into the heat sink.

cooled. The fibers protrude from a layer of a filler material (Cu, Ag, Au, or metal-particle-filled gels), which provides both mechanical support to maintain the carbon nanotubes in alignment and thermal conductivity to enhance the diffusion of concentrated heat from the nanotubes into the larger adjacent volume of a heat sink.

The array of carbon nanotubes, the filler material, and the heat sink are parts of a unitary composite structure that is fabricated as follows:

1. Using techniques that have been reported previously, the array of substan-

tially perpendicularly oriented carbon nanotubes is grown on a metal, silicon, or other suitable thermally conductive substrate that is intended to become the heat sink.

2. By means of chemical vapor deposition, physical vapor deposition, plasma deposition, ion sputtering, electrochemical deposition, or casting from a liquid phase, some or all of the interstitial volume between carbon nanotubes is filled with the aforementioned layer of mechanically supporting, thermally conductive material.

3. To cause the carbon nanotubes to protrude the desired length from the filler material, an outer layer of filler is removed by mechanical polishing, chemical mechanical polishing, wet chemical etching, electrochemical etching, or dry plasma etching.

This work was done by Jun Li of Ames Research Center and Brett A. Cruden and Alan M. Cassel of UARC.

Inquiries concerning rights for the commercial use of this invention should be addressed to the Technology Partnerships Division, Ames Research Center; (650) 604-2954. Refer to ARC-15173-1.



Pulse-Flow Microencapsulation System

Microcapsules are produced continuously under controlled, sterile conditions.

Lyndon B. Johnson Space Center, Houston, Texas

The pulse-flow microencapsulation system (PFMS) is an automated system that continuously produces a stream of liquid-filled microcapsules for delivery of therapeutic agents to target tissues. Prior microencapsulation systems have relied on batch processes that involve transfer of batches between different apparatuses for different stages of production followed by sampling for acquisition of quality-control data, including measurements of size. In contrast, the PFMS is a single, microprocessor-controlled system that performs all processing steps, including acquisition of quality-control data. The quality-control data can be used as real-time feedback to ensure the production of large quantities of uniform microcapsules.

A typical microcapsule produced by this system is a multilayered balloon between 10 and 200 μm in diameter. A microcapsule can contain an inner spheroid made of oil that serves as a dense radiographic contrast agent, surrounded by a thick shell of an aqueous drug solution, surrounded, in turn, by an outer polymer membrane or

wall. Optionally, the outermost liquid layer can also contain one or more ceramic ferromagnetic particles or other particles that can be activated by an externally generated magnetic or ultrasonic field to trigger the release of the therapeutic agent(s). Alternatively or in addition, the PFMS can be used to encapsulate live cells for transplantation, together with immobilized immunosuppressant agents that inhibit local immune rejection of the transplanted cells.

The PFMS (see figure) contains pumps, valves, and ultrasonic nozzles, all operated in coordination to produce multilamellar microcapsules in a continuous stream. The PFMS comprises five major subsystems:

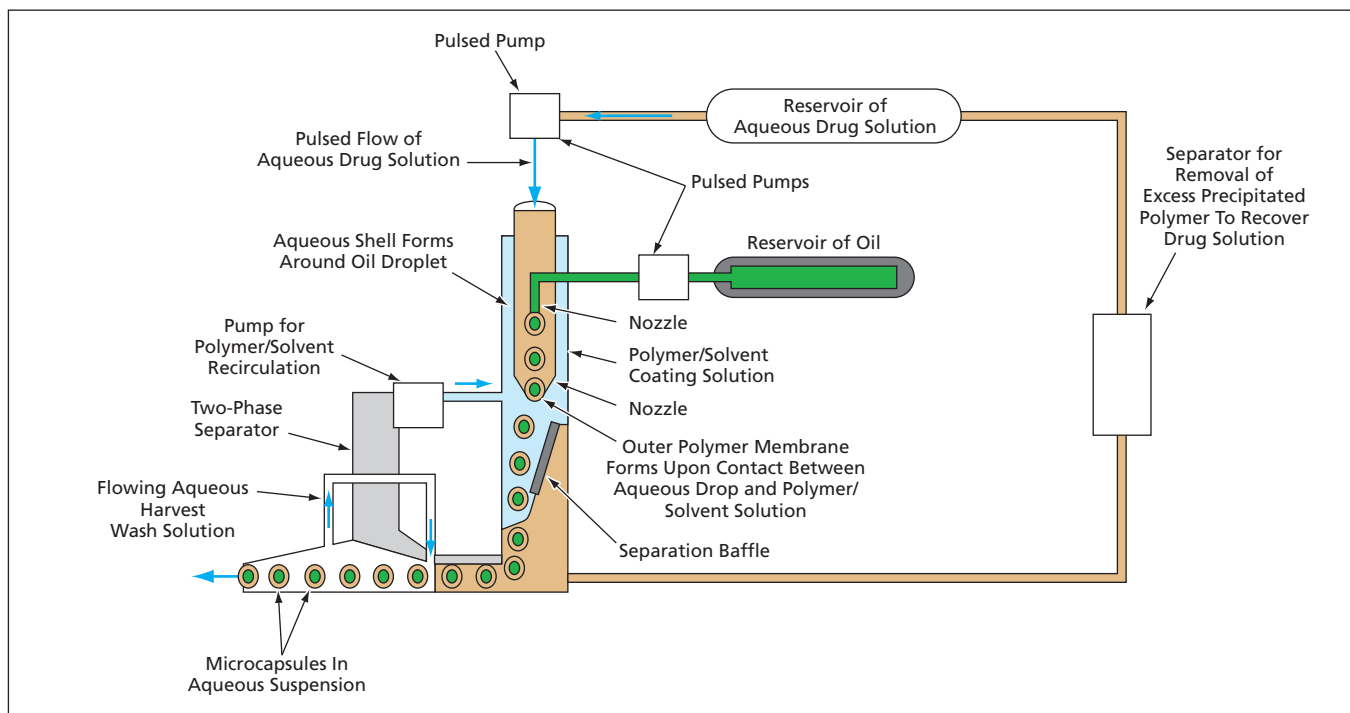
1. A pulse-flow, dual-nozzle microcapsule dispenser.
2. A sterile treatment flow module into which the liquid microcapsules are dropped to form their outer polymer walls.
3. A fluidized bed for washing and harvesting the microcapsules produced

by the combination of subsystems 1 and 2.

4. A microcapsule flow sensor, which acquires images of the microcapsules for quality control.
5. A microprocessor control module, which controls the operation of the pulse-flow microcapsule dispenser and the microcapsule flow sensor; logs the outputs of all sensors, including the microcapsule flow sensor; processes output of the microcapsule flow sensor to measure the sizes of the microcapsules, count the microcapsules, and distinguish between microcapsules and debris particles, which can be of about the same size; and effects feedback control of all pumps, ultrasonic transducers, and valves.

This work was done by Dennis R. Morrison of Johnson Space Center.

This invention is owned by NASA, and a patent application has been filed. Inquiries concerning nonexclusive or exclusive license for its commercial development should be addressed to the Patent Counsel, Johnson Space Center, (281) 483-0837. Refer to MSC-23659.



The Pulse-Flow Microencapsulation System generates a continuous flow of an aqueous suspension of multilamellar microcapsules.

Automated Low-Gravitation Facility Would Make Optical Fibers

Marshall Space Flight Center, Alabama

A report describes a proposed automated facility that would be operated in outer space to produce high-quality optical fibers from fluoride-based glasses, free of light-scattering crystallites that form during production in normal Earth gravitation. Before launch, glass preforms would be loaded into a mechanism that would later dispense them. A dispensed preform would be melted, cooled to its glass-transition temperature rapidly enough to prevent crystallization, cooled

to ambient temperature, then pushed into a preform tip heater, wherein it would be reheated to the softening temperature. A robotic manipulator would touch a fused-silica rod to the softened glass to initiate pulling of a fiber. The robot would pull the fiber to an attachment on a take-up spool, which would thereafter be turned to pull the fiber. The diameter of the fiber would depend on the pulling speed and the viscosity of the glass at the preform tip. Upon depletion of a preform, the robot

would place the filled spool in storage and position an empty spool to pull a fiber from a new preform. Pulling would be remotely monitored by a video camera and restarted by remote command if a break in the fiber were observed.

*This work was done by Dennis S. Tucker of **Marshall Space Flight Center** and Phillip J. Williams and Patrick A. Tobbe of *Dynamic Concepts*. Further information is contained in a TSP (see page 1).
MFS-31921-1*



Alignment Cube With One Diffractive Face

Only one theodolite is needed instead of two.

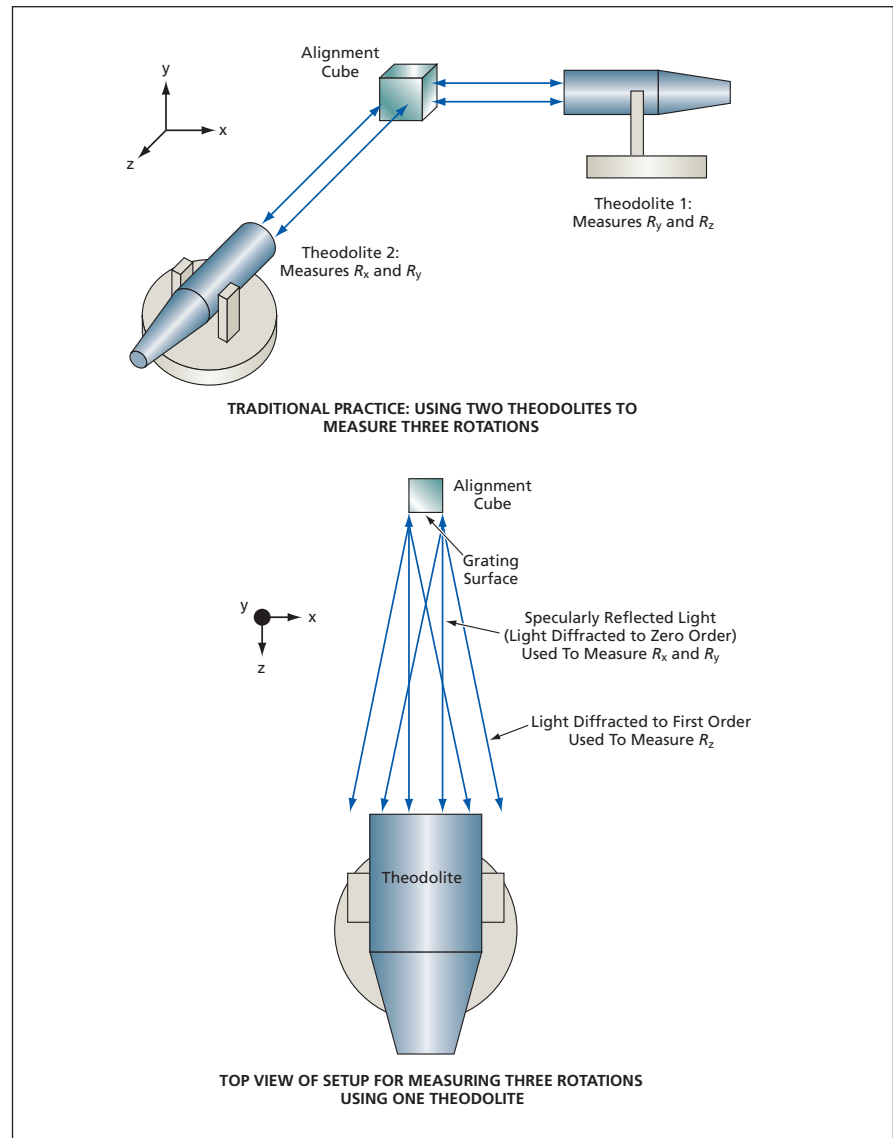
Goddard Space Flight Center, Greenbelt, Maryland

An enhanced alignment cube has been invented for use in a confined setting (e.g., a cryogenic chamber) in which optical access may be limited to a single line of sight. Whereas traditional alignment-cube practice entails the use of two theodolites aimed along two lines of sight, the enhanced alignment cube yields complete alignment information through use of a single theodolite aimed along a single line of sight.

Typically, an alignment cube is placed in contact with a datum surface or other reference feature on a scientific instrument during assembly or testing of the instrument. The alignment cube is then used in measuring a small angular deviation of the feature from a precise required orientation. Commonly, the deviation is expressed in terms of rotations (R_x, R_y, R_z) of the cube about the corresponding Cartesian axes (x, y, z). In traditional practice, in order to measure all three rotations, it is necessary to use two theodolites aimed at two orthogonal faces of the alignment cube, as shown in the upper part of the figure. To be able to perform such a measurement, one needs optical access to these two faces. In the case of an alignment cube inside a cryogenic chamber or other enclosed space, the optical-access requirement translates to a requirement for two windows located along the corresponding two orthogonal lines of sight into the chamber. In a typical application, it is difficult or impossible to provide two windows. The present enhanced version of the alignment cube makes it possible to measure all three rotations by use of a single line of sight, thereby obviating a second window.

Commercially available alignment cubes are usually made of glass or metal and have linear dimensions of about 1 in. (≈ 2.5 cm). The faces are reflective and highly polished and are orthogonal to within an angular tolerance of about 10 arc seconds. In traditional practice, one utilizes the specular reflections from the observed faces.

An alignment cube according to the present innovation is made from a commercially available alignment cube by forming a diffraction grating on the face



Two Theodolites are needed to measure rotations about all three Cartesian axes in traditional practice using a purely specular alignment cube. Applying a diffraction grating to one face of an alignment cube makes it possible to measure all three rotations using a single theodolite.

that is to be observed. This can be done either by using a ruling engine to machine grating grooves into the face or by attaching a replica grating to the face. The light from the theodolite striking this surface is diffracted into many orders. The light diffracted to zeroth order is the specular reflection; it gives the same alignment information (concerning the

rotations about the axes perpendicular to the line of sight) as does the light reflected from a traditional alignment cube. The light diffracted to higher orders creates additional image components in the theodolite field of view. The horizontal and vertical displacements of these components are related in a known way to the rotation about the line of sight. Hence, as

depicted schematically in the lower part of the figure, a single theodolite can be used to measure rotation about all three axes.

The amplitude and spatial period of the grating should be optimized for the peak wavelength (e.g. ≈ 540 nm) of the light source in the theodolite and for the viewing geometry as limited by the edge of the window (if any) in the intended application. Prior to use of the alignment cube, it is necessary to perform a calibration in

which the orientations of the remaining polished sides are measured with respect to the orientations of the specular reflection and the pertinent non-zero grating orders. If the cube is to be used during cryogenic operation, then the cube is placed in a small chamber at the anticipated operating temperature and the calibration is repeated. If these measurements show the calibration to be consistent in the presence of thermal

cycling, then the alignment cube can be used as described above to measure all three rotations.

*This work was done by Raymond G. Ohl, Henry P. Sampler, Carl R. Strojny, and John G. Hagopian of **Goddard Space Flight Center** and Joseph C. McMann of **ManTech International Corp.** Further information is contained in a TSP (see page 1).
GSC-14954-1*



Books & Reports

Graphite Composite Booms With Integral Hinges

A document discusses lightweight instrument booms under development for use aboard spacecraft. A boom of this type comprises a thin-walled graphite-fiber/matrix composite tube with an integral hinge that can be bent for stowage and later allowed to spring back to straighten the boom for deployment in outer space. The boom design takes advantage of both the stiffness of the composite in tubular geometry and the flexibility of thin sections of the composite. The hinge is formed by machining windows in the tube at diametrically opposite locations so that there remain two opposing cylindrical strips resembling measuring tapes. Essential to the design is a proprietary composite layout that renders the hinge tough yet flexible enough to be bendable as much as 90° in either of two opposite directions. When the boom is released for deployment, the torque exerted by the bent hinge suffices to overcome parasitic resistance from harnesses and other equipment, so that the two sections of the hinge snap to a straight, rigid condition in the same manner as that of measuring tapes. Issues addressed in development thus far include selection of materials, out-of-plane bending, edge cracking, and separation of plies.

This work was done by Wes Alexander, Rene Carlos, Peter Rossoni, and James Sturm of Goddard Space Flight Center. Further information is contained in a TSP (see page 1). GSC-14896-1

Tool for Sampling Permafrost on a Remote Planet

A report discusses the robotic arm tool for rapidly acquiring permafrost (RATRAP), which is being developed for acquiring samples of permafrost on Mars or another remote planet and immediately delivering the samples to adjacent instruments for analysis. The prototype RATRAP includes a rasp that protrudes through a hole in the bottom of a container that is placed in contact with the permafrost surface. Moving at high speed, the rasp cuts into the surface and loads many of the resulting small particles of permafrost through the hole into the container. The prototype RATRAP has been shown to be capable of acquiring many grams of permafrost simulants in times of the order of seconds. In contrast, a current permafrost-sampling system that the RATRAP is intended to supplant works by scraping with tines followed by picking up the scrapings in a scoop, sometimes taking hours to acquire a few grams. Also, because the RATRAP inherently pulverizes the sampled material, it is an attractive alternative to other sampling apparatuses that generate core or chunk samples that must be further processed by a crushing apparatus to make the sample particles small enough for analysis by some instruments.

This work was done by Gregory Peters of Caltech for NASA's Jet Propulsion Laboratory. Further information is contained in a TSP (see page 1). NPO-43128

Special Semaphore Scheme for UHF Spacecraft Communications

A semaphore scheme has been devised to satisfy a requirement to enable ultrahigh-frequency (UHF) radio communication between a spacecraft descending from orbit to a landing on Mars and a spacecraft, in orbit about Mars, that relays communications between Earth and the lander spacecraft. There are also two subsidiary requirements: (1) to use UHF transceivers, built and qualified for operation aboard the spacecraft that operate with residual-carrier binary phase-shift-keying (BPSK) modulation at a selectable data rate of 8, 32, 128, or 256 kb/s; and (2) to enable low-rate signaling even when received signals become so weak as to prevent communication at the minimum BPSK rate of 8 kHz. The scheme involves exploitation of Manchester encoding, which is used in conjunction with residual-carrier modulation to aid the carrier-tracking loop. By choosing various sequences of 1s, 0s, or 1s alternating with 0s to be fed to the residual-carrier modulator, one would cause the modulator to generate sidebands at a fundamental frequency of 4 or 8 kHz and harmonics thereof. These sidebands would constitute the desired semaphores. In reception, the semaphores would be detected by a software demodulator.

This work was done by Stanley Butman, Edgar Satorius, and Peter Illott of Caltech for NASA's Jet Propulsion Laboratory. Further information is contained in a TSP (see page 1). NPO-42910



National Aeronautics and
Space Administration